Pre-print: In *Free-Space Laser Communication Technologies XV*, G. Stephen Mecherle, Editor, Proceedings of the SPIE Vol. 4975, pp. TBD (2003).

Design and development of a robust ATP subsystem for the Altair UAV-to-Ground Lasercomm 2.5 Gbps Demonstration

Gerardo G. Ortiz*, Shinhak Lee, Steve Monacos, Malcolm Wright and Abhijit Biswas
Jet Propulsion Laboratory, California Institute of Technology
Pasadena, CA

ABSTRACT

A robust acquisition, tracking and pointing (ATP) subsystem is being developed for the 2.5 Gigabit per second (Gbps) Unmanned-Aerial-Vehicle (UAV) to ground free-space optical communications link project. The demonstration will gather HDTV images of regions of geological interest (e.g. volcanic) and then downlink those images to ground receivers at a range of 50 km while the UAV is at an altitude of 18 km. With a 200 mW downlink laser at 1550 nm for a BER of 1E-9, the pointing requirements on the flight terminal are a jitter error of 19.5 urad and a bias error of 14.5 urad with a probability of pointing induced fades of 0.1 %. In order to mitigate the effect of atmospheric fades and deal with UAV flight and vibration uncertainties (relatively new craft) the ATP subsystem requirements have been set to a stringent level in order to assure success of the communication link. The design, analysis and development of this robust ATP subsystem will be described in this paper. The key innovations that have been developed to make the ATP subsystem robust are i) the application of inertial sensors to make the acquisition and tracking functions tolerant to atmospheric fades, ii) the usage of active exposure control to provide a 16 dB dynamic range on the Focal Plane Array (FPA) tracking window, and iii) the introduction of a second ultra wide field of view camera to assure acquisition of the ground beacon.

Keywords: Free-space optical communications, UAV-to-Ground Lasercomm, high rate comm

1. INTRODUCTION

JPL's Optical Communications Group is developing a bi-directional daytime and nighttime optical communications link from an Altair UAV to stationary ground stations located at TMF, Wrightwood, CA and AMOS, Maui, HI. The link demonstration utilizes existing NASA/DOD optical ground stations (NASA OCTL in southern California, USA Air Force AMOS in Hawaii) to leverage prior government investment in optical ground stations. The demonstration is hosted on a moving aerial platform (a jet version of the General Atomics Predator Unmanned Aerial Vehicle (UAV) of particular interest to the sponsoring community) for ultimate deployment of the proven Lasercomm capability. The flight lasercom terminal, the Optical Communications Terminal (OCT), design is based on the NASA/JPL-developed Optical Communications Demonstrator (OCD) lasercom terminal [1] to leverage substantial, prior government investment in the development of lasercom technology.

A key aspect of the OCT design focuses on making the ATP functions robust in their performance. The robustness has been built into the system by the introduction of an auxiliary wide field of view camera, an increased 16 dB dynamic range requirement for beacon tracking and the application of inertial sensors to mitigate the effects of atmospheric fades [2]. This paper will present an overview of the project and mission and will then present the design, analysis and development of the ATP Subsystem.

* Gerry.G.Ortiz@jpl.nasa.gov; http://opticalcomm.jpl.nasa.gov

2. 2.5 GBPS UAV-TO-GROUND LASERCOMM PROJECT OVERVIEW

2.1. Optical Link Configuration

The demonstration of the free-space optical communications link is outlined in figure 1. The UAV is commanded to take science images over desired targets (e.g. volcanoes in Hawaii) and then downlink the images thru the optical communications channel. Optical communications is initiated by the Optical Communications Terminal (OCT) receiving a command from ground via one of Altair's standard RF links. The terminal also receives continuous updates of the GPS information being collected by the UAV GPS receiver. The UAV also provides the OCT with its GPS/INS information. The terminal uses this information with a priori knowledge of the ground location to blind point the gimbal. At this time, the ground has now illuminated the aircraft with the beacon signal. The flight terminal tracks on the beacon signal and begins data communications until the data transfer is complete.

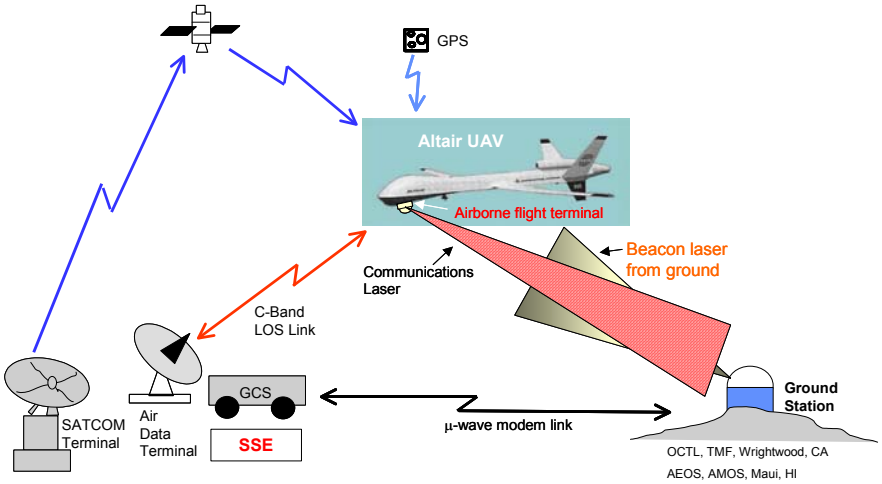

Figure 1. Project objective is to demonstrate a bi-directional daytime and nighttime optical communications link from an Altair UAV to stationary stations located at TMF, Wrightwood, CA and at AMOS, Maui, HI.

The baseline plan is to utilize the Altair UAV as the aerial platform for demonstrating a high data rate optical communications air-to-ground link to a stationary ground station. The plan is to replace the payload normally flown in the gimbal assembly with the optical communications payload. The Altair is an un-manned aerial vehicle (UAV) that can be used for military reconnaissance, scientific research and commercial applications. It has a wingspan of 25.6 m, length of 11 m and a height of 3.6 m [3]. It has a total payload capacity of 297 kg and a payload volume of 155 m^3. The Altair UAV is remotely piloted using a C-band line-of-sight, or an Over-the-Horizon Ku-band data link. The Altair cruise speed is nominally 70-100 m/s (144-200 Knots) true air speed at an altitude of 15.8 – 18.3 Km (52-60 Kft). The Altair UAV provides INS/GPS data through an RS422 interface to OCT at an update rate no less than 1 Hz with an attitude knowledge accuracy of < 0.05 degrees in pitch and roll and 0.10 degrees in yaw (true heading) and position knowledge less than +/- 10 m CEP. The aircraft's in-flight vibration spectra during cruise mode, at the OCT mounting point, is expected to be as specified for "LOC A FWDBAY" in the Predator Flight Test Data/Analysis Tesar Vibration Report (Westinghouse, Sept 23, 1994). The true angular vibration for the Altair vehicle will be characterized prior to the mission utilizing the vibration sensor package described below. The aircraft has an attitude flight stability (deviations in pitch, roll and yaw) within +/- 1 degree and a maximum rate change < 5 degrees/sec.

The UAV altitude is in the range of 15.8 km to 18.3 km. The laser footprint on the ground needs to be greater than 1.5 m at TMF and 3.0 m at AMOS to ensure non-obstruction by the secondary of the telescope. The laser footprint at the flight terminal on the UAV needs to be greater than 10 m due to position uncertainty. The maximum zenith angle at TMF is 70 degrees while at AMOS it is 85 to 90 degrees. Because of these constraints the possible link range varies between 15 km

and 100 km depending on the zenith angle. The range goal for this project is 50 km, which would require operation at a zenith angle of 75 degrees.

2.2. Mission plan

The mission scenario for the UAV is driven by the science gathering requirements and the optical communication downlink requirements. The baseline science mission for the UAV involves imaging of interesting ground morphologies such as volcanic regions in central California or on the big island of Hawaii and storing the data for transmission during the downlink opportunities to the ground receivers. The instrument used is a high definition video camera (HDTV) in a progressive scan mode with a high-speed serial output signal. The camera can also be used for real-time imaging and transmission during the downlink portion of the flight path.

Due to the line of sight requirement of optical communication the UAV must follow a flight path around the ground receiver station to downlink the collected data, see figure 2. A circular path at fixed altitude requires only azimuthal tracking once acquired. There are several factors that constrain the flight path of the UAV during the downlink of the flight. The UAV flies at a specific altitude that is determined by the imaging requirements as well as the aircraft performance envelope. The link range to the ground station is basically determined by the flight laser power along with the ground telescope constraints. Taking into account all the link parameters including telescope aperture and receiver efficiency produces a link range of 32 km as a design point. The maximum distance is determined by how large the ground telescope's zenith angle can be made. This in turn is limited by ground obscurations at the telescope site such as trees or nearby mountain ridges. For the OCTL facility, an optimum flight path of 25 degrees in elevation (zenith angle of 65 degree) is required. Since some of the downlink opportunities are during the day, the telescope solar avoidance angles have to be taken into account. This is particularly important during a dawn or evening link time when the sun can be directly behind the UAV. The telescope must then break and re-acquire the link within this +/- 30 degrees. The azimuthal slew rate of the telescope must also be able to maintain tracking of the aircraft. Given the aircraft nominal speed of 320 km/hr and link range of 32 km (20 km radius loop) the maximum slew rate of 20 degrees/sec is sufficient to maintain link. However, the telescope has a maximum travel distance of +/-335 degrees so once this is reached it must break the link and reverse or unwind and reacquire the aircraft. To test out a real operational scenario, a racetrack or figure eight flight path with the telescope centered on one loop or one end of the racetrack path is desired in order to have multiple flight and ground terminal acquisitions.

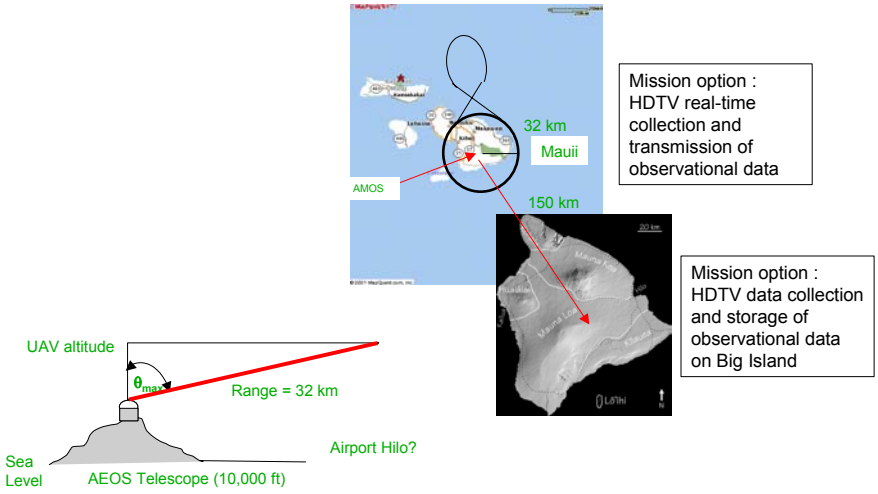

Figure 2. Mission scenario for optical communications demonstration at Hawaii.

The other main factor in the operational scenario is the actual time of flight. The UAV is sensitive to wind speed at altitude due to bank angle requirements and the ability to maintain a line of sight during bank between the flight terminal and ground station. This also affects the chosen altitude. Based on wind conditions that have been characterized at Edwards AFB, just north of the OCTL facility, and in Kauii, Hawaii, late summer and early autumn seem the optimal

time of year for the optical communication experiment with flights beginning in the middle of the night and continuing through early morning to cover a wide variety of link conditions.

2.3. Atmospheric channel effects

The uplink beacon received by the 10 cm aperture flight terminal will be prone to atmosphere turbulence induced irradiance fluctuations. These are characterized by the normalized variance of irradiance or scintillation index (SI). For example, an SI of 0.4 will give rise to a 3.6E-5 probability of 12 dB fades. The corresponding mean duration of these fades is approximately 2 ms. Approximately one fade in 50 seconds occurs during a cross-wind with a speed of 3 m/s. The beacon beam arriving at the terminal will be prone to high frequency (50-100 Hz) and low frequency (<10 Hz) angle of arrival fluctuations. The estimated RMS high frequency angle of arrival fluctuations for the uplink beam is of the order of 1 urad. The estimated low frequency beam wonder is approximately 18 urad.

On downlink, irradiance fluctuations will be mitigated by large aperture averaging factors > 0.08 for the 1-m telescope and 1550 nm. Atmospheric 'seeing' will cause blurring of the focal spot size on the downlink beam. The nominal blur circle size from 1550 nm is 70 um. The worst-case blur circle size is estimated to be 200 um, which may result in truncation loss at the detector.

2.4. Downlink Analysis Summary and Pointing Budget

There is a large link margin while transmitting with the 200 mW (+23 dBm) peak power laser at 1550 nm for a BER of 1E-9 at 2.5 Gbps. The system loss is estimated at 14.3 dB, the pointing loss at 4.2 dB and other losses at 9 dB. The required power at the receiver is –30 dBm, thereby resulting in a link margin of 26 dB at TMF. With slightly lower losses at AMOS the link margin is 27 dB when communicating to AMOS.

The overall pointing budget is presented in Table 1. This budget has been allocated to meet the nominal pointing loss requirement of 4.2 dB. The allocations have been made to account for the expected performance of each of the components. The downlink beam-width is 200 microradians. The total pointing requirements on the flight terminal are a jitter error of 19.5 urad and a bias error of 14.5 urad with a probability of pointing induced fades (PIF) of 0.1 %. The ATP Subsystem has been designed to meet these performance requirements.

UAV Lasercomm Demo Overall Pointing Budget			
Error Source	Jitter (urad)	Bias (urad)	
Optical Comm. Terminal			
Acquisition Tracking and Pointing	18.6	2.2	
Telescope	2.0	10.0	TBR. Mechanical misalignment, thermally induced misalignments
Laser	0.5	0.5	TBR. Beam co-alignment drift, intensity fluctuations.
Atmosphere			
Phase Tilt - high frequency	1.0	0.0	TBR. Causes phase tilt changes of uplink beacon
Phase Tilt - low frequency	0.5	TBD	TBR. Causes phase tilt changes of uplink beacon
Intensity fluctuations	0.5	0.0	TBR. Causes intensity fluctuations of uplink beacon at FPA
Ground System			
GS Pointing Jitter	2.0	2.0	TBR. Causes intensity fluctuations of uplink beacon at FPA
Design Margin			
	5.0	10.0	
Total RSS (urad)	19.5	14.5	

Table 1. UAV Lasercomm Demonstration Overall Pointing Budget.

2.5. The Optical Communications Terminal (OCT)

The airborne flight terminal is called the Optical Communications Terminal (OCT) and is being developed for demonstrating high rate optical communications from a UAV to a stationary ground station. It is based on the NASA/JPL OCD legacy design with improvements and modifications. The design architecture, with minor modifications, can support UAV-to-UAV, aircraft, GEO and LEO satellite links. Furthermore, with flight qualification it

can support LEO-to-Ground and LEO-to-GEO optical links. The OCT is comprised of the following functional elements: i) the laser transmitter subsystem (LTS), ii) the transceiver optics subsystem (TOS), iii) the acquisition, tracking and pointing subsystem (ATPS) and the iv) the electronics processor subsystem (EPS). For the UAV demonstration the functional units are physically distributed into i) the Turret Assembly, ii) the Electronics Box and iii) the umbilical cord that runs between them (see figure 3). The Optical Transceiver is integrated to the Turret Assembly (Gimbal) and the Electronics box is connected via an Umbilical Cord. The Electronics box resides in the payload bay of the UAV while the Turret Assembly is mounted in the underbelly of the aircraft. The OCT weight is base-lined at 42 kg for the turret and 25 kg for the electronics box. The power consumption of the OCT is 650 W.

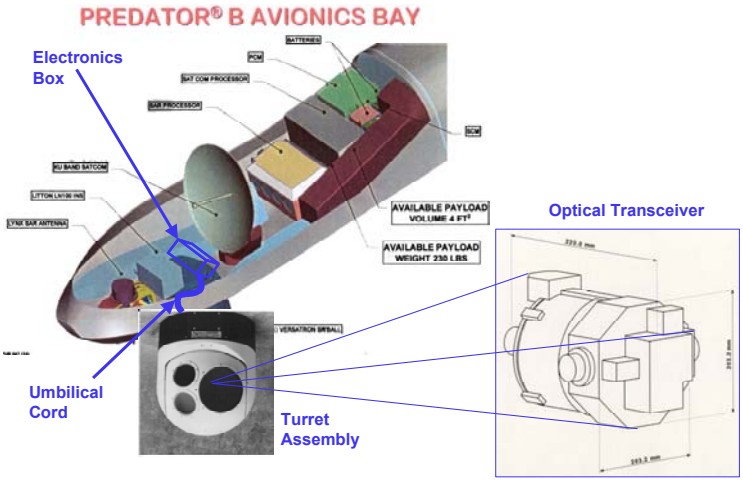

Figure 3. Integration of the Optical Communication Terminal to the UAV.

3. ATP SUBSYSTEM DESIGN AND ANALYSIS

3.1. Description

The Acquisition, Tracking and Pointing Subsystem (ATPS) is composed of six assemblies responsible for acquiring and tracking the beacon laser from the ground terminal receiver and accurately pointing the downlink transmit laser to the receiver. The assemblies are the Wide Field of View (WFOV) Camera, the Narrow Field of View (NFOV) Camera, the Coarse Pointing Assembly (CPA), the Digital Control Assembly (DCA), the Accelerometer Sensor Assembly (ASA) and the Fast Steering Assembly (FSA).

The typical operation of the ATPS is as follows and illustrated in figure 4. Upon a command from the UAV to begin acquisition, the ATPS receives GPS/INS information from the UAV, which it uses, along with a priori knowledge of the Ground Terminal location, to blind point the CPA in the direction of the Ground Terminal. At this point the Ground Terminal is tracking the UAV and illuminates it with the 810 nm beacon signal. This beacon is imaged onto the FPA of the WFOV Camera, which samples the image and locates the beacon spot. The OCT autonomously acquires the beacon laser provided the mean irradiance falls within the range of 4e-10 +/- 1.3e-10 W/cm^2. Using this centroid information, the CPA is commanded to track the beacon and the tracking loop is closed. After illumination of a proper level intensity by the beacon, closed-loop tracking initiates within 10 seconds. The CPA is commanded to maintain the LOS with the beacon, which maintains the beacon in the center of the WFOV Camera's FPA. The NFOV Camera is optically co-aligned with the WFOV Camera. This ensures that, when the coarse pointing system is tracking, the ground beacon enters and is focused onto the FPA of the NFOV Camera. At this point the beacon spot is acquired and tracked in the NFOV Camera. Simultaneously, the transmit reference beam is focused onto the same FPA. This beam's spot is also acquired and tracked. An error signal is computed between these two spots and sent to the Fine Steering Mirror (FSM) to close the fine pointing loop. Information from the accelerometers is also used in the fine tracking loop to compensate for micro-vibrations and mitigate the effect of beacon fades on tracking and pointing of the transmit beam.

The ATPS points the communication laser to the ground station with an RMS jitter not to exceed 18.6 urad and a bias error not to exceed 2.2 urad. This performance is expected provided the UAV platform vibration is within the specified power spectral density (PSD) envelope. ATPS is compatible with operating in the presence of earth-reflected radiance not exceeding 70 uW/cm^2 sr-nm transmitted through an optical filter centered at 810 nm and with a spectral bandpass of +/- 2.5 nm.

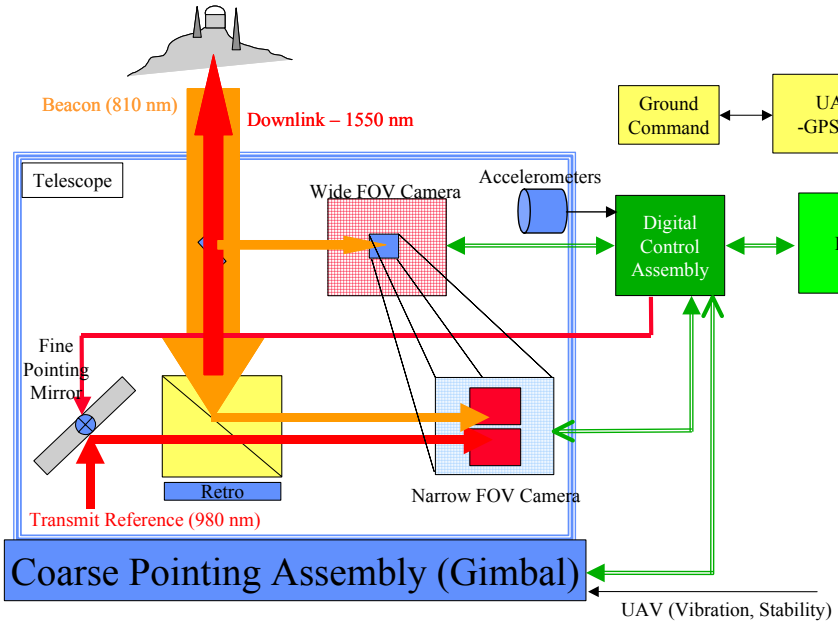

Figure 4. Description of the Acquisition, Tracking and Pointing Subsystem (ATPS).

3.2. Coarse Control Loop

The proposed mode of operation for acquisition and tracking using both wide field-of view (WFOV) and narrow field-of-view (NFOV) cameras with a gimbal, shown in figure 5, is as follows. Positional information from the GPS system will be used to initially point the gimbal towards the ground-based receiver. This information is used to open loop point the gimbal well within the 3 degree WFOV camera. With the beacon in the WFOV, the gimbal control will switch from open loop pointing to closed loop pointing using optical feedback from the WFOV camera. The gimbal criterion during this transition is the response time of the gimbal versus the number of pixels that can be traversed by the beacon during this period. The gimbal response time is a combination of the update time and the transient response of the gimbal. For a 30 Hz gimbal update rate, the update time is 33 ms. The transient response of the gimbal needs to be measured for a step input to determine the time it takes to achieve 90% of the desired motion. The transition is successful if the beacon is still within the WFOV. The gimbal pointing error can be up to 0.30 mrad due to the 30 Hz gimbal update rate. If we factor in the gimbal static pointing uncertainty, the total gimbal pointing error is 0.335 mrad in the worst case and corresponds to 8.2 pixels in the NFOV. This result means that the differential motion of the beacon with respect to the NFOV will be up to 8 pixels due to the 33 ms delay in controlling the gimbal and pointing inaccuracy. For a 50 Hz update rate, the corresponding gimbal pointing uncertainty will be 0.215 mrad or 5.3 pixels.

The consequence is that the gimbal control inputs must position the gimbal to keep the beacon at least 8 pixels (out of 480x480) from the edge of the NFOV to avoid losing the beacon with a 30 Hz gimbal update rate. For a 50 Hz update rate, only 5 pixels are required. The fine tracking loop can use the entire FOV for beacon tracking but the coarse tracking loop is required to control the gimbal such that the beacon will stay within the clear area in the NFOV. This means that the next control inputs must move the gimbal far enough such that the current beacon position will be at least 8/5 pixels away from any edge of the NFOV depending on the gimbal update rate.

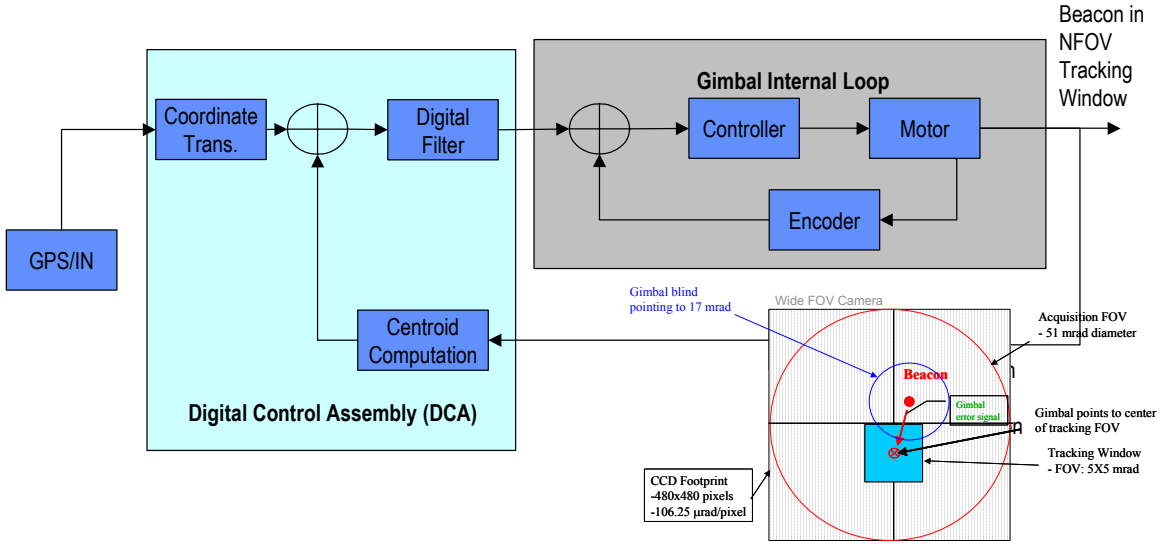

Figure 5. Coarse Control Loop Diagram with Wide Field of View Camera FPA.

3.3. Fine Control Loop Diagram

The fine control loop's major function is to compensate for the UAV's micro-vibrations. It does this by tracking the ground beacon computing the error vector between the pointed direction and the received beacon direction and commanding the steering mirror to correct the error as seen in figure 6a. Tracking of the beacon and transmit beam spots is done with the fast region of interest, windowing CCD camera [4] developed at JPL. The expected vibration, shown in figure 6b has been taken from the Experimenter's handbook. Because the data provided is linear vibration a translation was done to angular vibration based on the mounting location of the OCT. The resulting disturbance rejection is shown also in figure 6b, with at total residual tracking error of 15 urad.

The accelerometers are used in the fine control loop for two purposes. The primary purpose is to mitigate the effects of atmospheric fades (see section 3.5) and the secondary purpose is to extend the rejection bandwidth of the compensation control loop.

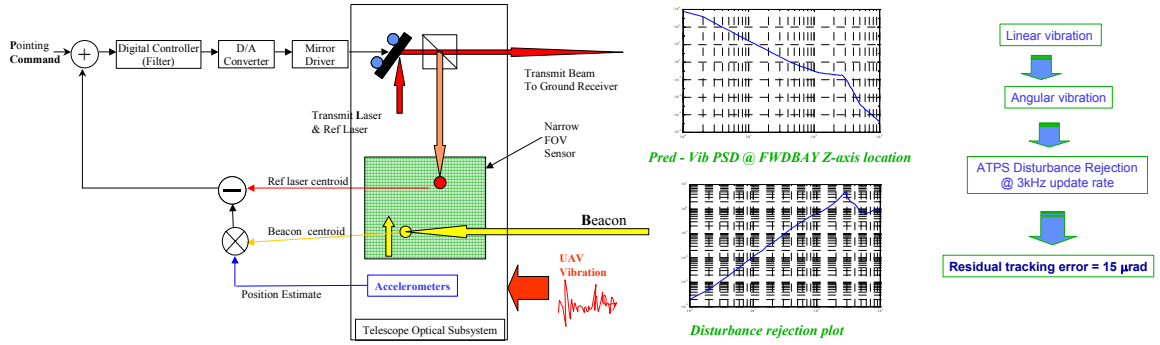

Figure 6. a) Fine control loop diagram, b) UAV Vibration PSD, and c) disturbance rejection plot.

3.4. 16 dB of Dynamic Range

For the UAV optical communications demonstration, a 13 dB dynamic range is the requirement with the goal of 16 dB for the CCD tracking window. Atmospheric effects such as scintillation and beam wandering drive this dynamic range requirement. The two constraints to design for this dynamic range are a) the minimum beacon signal requirement

(15,000 e-) for tracking accuracy and, b) the CCD pixel full well of ~30,000e-. A signal level of 13 dB and 16 dB above 15,000 electrons is 300,000 and 600,000, respectively.

Two methods, beam broadening and exposure control, can deliver the desired dynamic range given the two constraints. The beam broadening method impacts the optical design whereas the exposure control method can be implemented with either software or electric shutter.

The beam broadening method is a natural solution to resolve the three conflicting constraints: a) minimum signal of 15,000 e-, b) pixel full well limit of 30,000 e-, and c) the required dynamic range of 13 dB. Consider the simple case of the beam focused on only one pixel. This results in a 3 dB dynamic range (15,000 e- to 30,000). Now broaden the spot to cover a 4x4 pixel area, which results in a 9 dB (15,000e- to 120,000e-) dynamic range, assuming the beam is uniformly distributed. In a similar fashion the beam spot size can be broadened until a size is reached that will meet the constraints. In reality, the beam is not uniformly distributed; this drives the design to have a larger beam size. Nonetheless, the analogy works. Using a Gaussian beam profile, a 7x7 beam would meet the 16 dB dynamic requirement, and a 5x5 would provide a 13 dB dynamic range as shown in figure 7.

An alternative solution is the straightforward approach of using exposure control. By controlling the incoming light, we can minimize the beam intensity fluctuation while it meets the minimum signal requirements. This method is more flexible since it can be easily implemented and provides greater dynamic range. Two possible implementation methods are available: S/W approach and electric shutter approach. One critical aspect to be checked is the effect of frame transfer time period on the centroid accuracy. When the exposure time is close to the frame transfer time, we expect that the centroid accuracy would be affected significantly. Total frame transfer time (500 rows) is assumed to be 50 microseconds. Each row will take 1/500th of a 50 microsecond (usec) period. During the frame transfer from sensor to storage area, the CCD pixels are exposed to the signal beam. This exposure time although small will produce a ghost image, which will cause a bias error in the centroid. The analysis demonstrated the effect of frame transfer is minimal as shown in figure 8. The exposure can be from around 50 usec to a longer period, depending on the update rate allowed. For example, if we take from 50 usec to, for example, 1 msec, then about 13 dB can be obtained. Photons collected in the centroid window are proportional to the exposure time to result in a ratio of 1 to 20, which gives 13 dB.

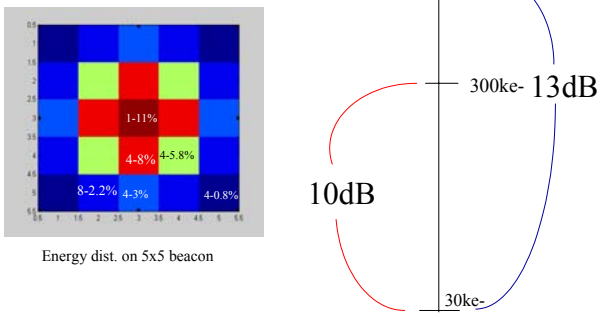

Figure 7. Beacon Energy distribution on CCD exemplifying large dynamic range operation.

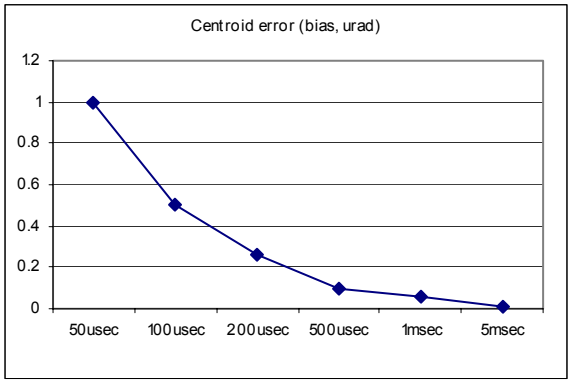

Figure 8. Centroid error (bias, urad) vs. exposure time

Given the difficulty to meet certain beam size requirements from the standpoint of optical design, it might be effective to combine both the optical design approach (beam broadening) and S/W exposure control. This way, a margin of tolerance can be given to the optical design while the 16 dB dynamic range can be easily met with S/W exposure control. Furthermore, careful use of this exposure control may bring extra dynamic range beyond the requirement.

3.5. Atmosphere Tolerant ATP

In any optical beacon based pointing system whose beacon travels through the atmosphere, atmospheric induced fade occurs with various fade periods depending on the driving phenomenon. During such fade periods, the tracking terminal looses the line-of-sight due to the dimmed/blocked beacon. Consequently, data transmission is interrupted until reacquisition of the beacon and handover to tracking is completed. Over the whole communication period there may be many fades each of which results in lost communication time. As the number of fades increases, the average data rate decreases, thereby, requiring an increase in the transmission period to complete transfer of the data volume. This problem is exacerbated for high data rate (Gigabit/second) optical communications systems, where a short (millisecond) fade may loose Megabits of information per fade.

This design introduces an innovative solution to atmospheric induced fades by using high bandwidth inertial sensors in the tracking loop. The key principle is to measure the platform vibrations, which is the most dominant disturbance to the beacon motion on the CCD detector, and use it to map the beacon position on CCD. This information is used to continue pointing the transmit laser towards the receiver and therefore continue the data transmission without any interruption. The duration that the pointing can be maintained without the presence of beacon on the detector depends on the fade period. While a typical atmospheric fade period is on the order of 1 millisecond, the maximum duration that the inertial sensors can keep accurate pointing ranges up to 30 milliseconds without affecting pointing accuracy. This tracking and pointing can last longer if the pointing accuracy is relaxed. Further analysis of this new system has also shown that it can maintain track, before needing to re-acquire, beyond 3 seconds [1].

As shown in Figure 9, if the angular displacement estimation error is limited to 1 urad, the duration of accurate pointing in the presence of a fade is 25 milliseconds. The maximum duration before tracking loss and re-acquisition is begun is 3 sec. This case corresponds to the beacon being centered in the narrow field-of-view. Depending on the fade duration, this analysis indicates that application of accelerometer information mitigates mis-pointing and tracking loss caused by beacon fades.

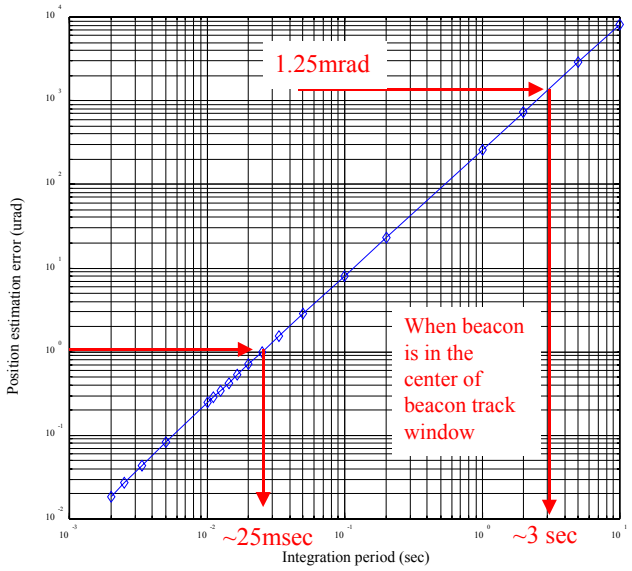

Figure 9. Position estimation error vs. duration (integration time).

3.6. Pointing Jitter Budget

Table 2 represents the allocations of the pointing jitter to the expected error sources. An analysis of the designed system has been carried out to assess whether the design meets the overall requirement. The analysis details are presented throughout this paper in support of the design.

Jitter Error Sources	*Allocations*		*Analysis*
Beacon NEA	5.0		4.5
Spatial quantization	1.0		0.7
Non-uniformity	0.6		0.5
Reference beam NEA	1.4		1.2
Spatial quantization	0.5		0.2
Non-uniformity	0.6		0.5
Vibration residual	16.0		15.0
Gimbal	6.0		5.0
Accelerometer	5.0		4.0
Total (urad)	18.6		17.0
Bias Error Sources	2.2		2.0
Point ahead	1.0		0.9
Accelerometer bias	2.0		1.8

Table 2. ATPS Pointing Jitter Budget with estimates from analysis.

Beam size and beam profile affect pointing jitter in terms of spatial quantization error that is part of centroid error. Estimates on both the transmit reference and beacon beams are now given. The transmit reference beam is assumed to be based on sub-aperture approach and the beacon beam is from aberration approach. Presently, the size of transmit reference beam (1/e^2) was selected as 70 um on the FPA for the transmit beam divergence of 200 urad. For the beacon beam the size is not yet finalized but is expected to be in the range of 40 – 60 um. The transmit reference beam is about 10x10 pixels and the centroid window of 15x15 pixels was used. The resulting spatial quantization error is 0.009 pixels. For the design of 20 urad/pixel, the error is 0.18 urad. Due to its large beam and smooth gaussian beam profile, the error is relatively small. The beacon beam profile is not smooth due to aberration applied in order to increase the beam size as shown in figure 10. The corresponding spatial quantization error is larger than that of the transmit reference beam and gradually increases as its size decreases from 60 um to 40 um, from 0.03 to 0.034 pixels. For this pixel resolution the beacon beam spatial quantization error is estimated from 0.60 to 0.68 urad.

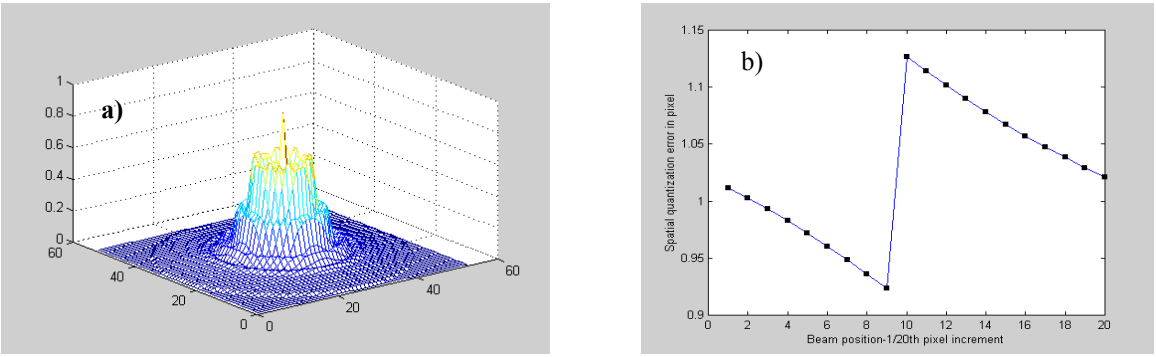

Figure 10. a) Beacon beam profile (40 um), 13x13 pixels shown and b) 1 sigma error of 0.68 urad with a centroid window of 9x9 pixels.

4. ATPS DEVELOPMENT

4.1. Breadboard Integration

The ATPS system is currently in the breadboard development phase. Four of the assemblies have been mechanically integrated as can be seen in figure 11. These are the NFOV CCD Camera [5], the DCS, the ASA and the FSA. The CPA is currently being obtained. Figure 12 shows the transmit reference spot on the NFOV Camera showing a spot size of approximately 6.5 by 8 pixels (48.1 by 59.2 um).

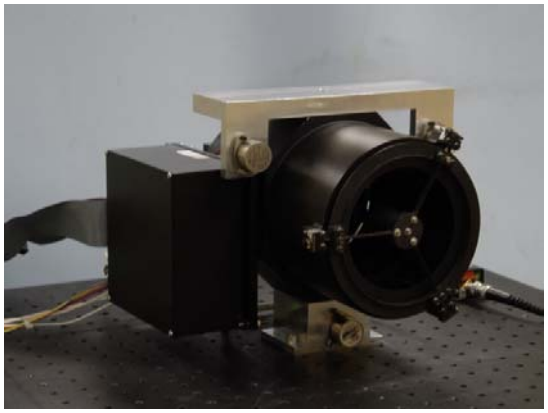

Figure 11. Breadboard of the ATP Subsytem.

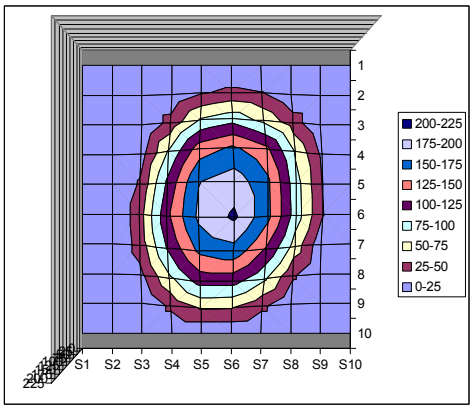

Figure 12. Example of the transmit reference beam spot on the NFOV CCD camera with a 9x9 centroiding window.

4.2. Flight Terminal Platform Vibration PSD Testing

In order to provide a better design of the vibration compensation control loop the angular vibration power spectral density (PSD) of the Altair UAV at the Turret mounting point will be obtained thru direct measurement. This is being measured with a JPL-built Angular Vibration Test Fixture (AVTF), as shown in figure 13. The fixture contains three angular rate sensors, three accelerometers and a temperature sensor. All sensors are mounted in an orthogonal orientation, thereby providing a six-degree of freedom sensor platform. Assembly of the AVTF and characterization of the sensor transfer functions has been completed. A sample transfer function is shown in figure 14 for the ARS-12 (angular rate sensor) after mounting in the fixture. Data is sampled and stored in a battery operated control system that is triggered by a pressure sensor set to go on at a prescribed altitude.

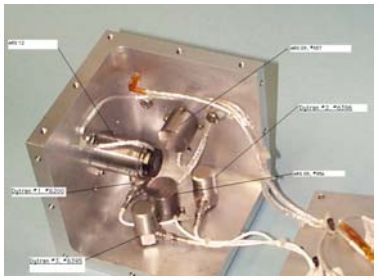

Figure 13. JPL's Angular Vibration Test Fixture.

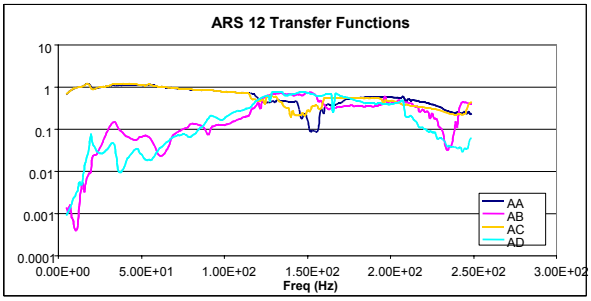

Figure 14. Transfer function of one of the angular rate sensors.

SUMMARY

A robust acquisition, tracking and pointing (ATP) subsystem has been presented. This subsystem is being developed for the 2.5 Gigabit per second (Gbps) Unmanned-Aerial-Vehicle (UAV) to ground free-space optical communications link project. Analysis has been presented to demonstrate that the system meets the allocated pointing requirements of a jitter error of 18.6 urad and a bias error of 2.2 urad. In order to mitigate the effect of atmospheric fades and deal with UAV flight and vibration uncertainties, the ATP subsystem has also implemented some key innovations that have been developed to make the ATP subsystem robust. These are i) the application of inertial sensors to make the acquisition and tracking functions tolerant to atmospheric fades, ii) the usage of active exposure control to provide a 16 dB dynamic range on the FPA tracking window, and iii) the introduction of a second ultra wide field of view camera to assure acquisition of the ground beacon.

ACKNOWLEDGEMENTS

The work described was funded by the BMDO and performed at the Jet Propulsion Laboratory, California Institute of Technology under contract with the National Aeronautics and Space Administration.

REFERENCES

[1] D. Russell, H. Ansari, C.-C. Chen, "Lasercom pointing, acquisition and tracking control using a CCD-based tracker," in *Free-Space Laser Communication Technologies VI*, G. Stephen Mecherle, Editor, Proceedings of the SPIE Vol. 2123, pp. 294-303 (1994).

[2] S. Lee and G. G. Ortiz, "Atmosphere tolerant Acquisition, Tracking and Pointing Subsystem," in *Free-Space Laser Communication Technologies XV*, G. Stephen Mecherle, Editor, Proceedings of the SPIE Vol. 4975, pp. TBD (2003).

[3] "Altair Experimenter's Handbook" by General Atomics Aeronautical Systems, Inc, document # ASI-00194B, August 27, 2001.

[4] S. P. Monacos, R. K. Lam, A. A. Portillo and G. G. Ortiz, "Design of an event-driven random-access-windowing CCD-based camera," in *Free-Space Laser Communication Technologies XV*, G. Stephen Mecherle, Editor, Proceedings of the SPIE Vol. 4975, pp. TBD (2003).

[5] W. Farr, B. Liu and S. P. Monacos, "Characterization of the random-access-windowing CCD camera for optical comm ATP Subsystem," in *Free-Space Laser Communication Technologies XV*, G. Stephen Mecherle, Editor, Proceedings of the SPIE Vol. 4975, pp. TBD (2003).